Optical Tweezers

BGGN 266, Biophysics Lab

June, 2009

Trygve Bakken & Adam Koerner

Background

There are a wide variety of force spectroscopy techniques available to investigators of biological systems. Atomic force microscopy (AFM), micro-needle manipulation, and magnetic and optical tweezers, among other techniques have enabled researchers to manipulate objects with exquisite spatio-temporal resolution. Each of these techniques has its niche uses, but optical tweezers are arguably the most flexible because of their fine control over a wide range of applied forces, and their ability to precisely measure 3D motion of anything from small molecules to whole living cells. In contrast, AFM has less spatial and temporal sensitivity to the motion of a tethered object, but can exert much larger forces and can be scanned across the surface of a material to generate a map of surface features.[1]

	Optical tweezers	**AFM**
Spatial resolution (nm)	0.1–2	0.5–1
Temporal resolution (s)	10^{-4}	10^{-3}
Force range (pN)	0.1–100	10–10^4
Probe size (μm)	0.25–5	100–250
Limitations	Photodamage Sample heating Nonspecific	Large high-stiffness probe Large minimal force Nonspecific

Optical tweezers have a long history in theoretical and experimental physics. In the 17th century, Kepler speculated about the radiation pressure of light from the tails of comets, and 150 years later Maxwell predicted the pressure from electromagnetic radiation. In the early 20th century, Ledebew, Nichols and Hull performed the first experiments observing this pressure.[2] But not until 1969 did Arthur Ashkin realize that this pressure, though a small force, could be useful to trap

small particles. He trapped dielectric spheres with radiation and gravitational forces [3], and in 1986, he trapped a particle with the gradient force of a single laser beam.[4]

Physical theory

While a complete description of optical tweezers requires Maxwell's equations of electromagnetism, we can get a good intuition of the physics involved by resorting to approximations. First, we will consider trapping of a small dielectric sphere with a radius a much greater than the incident laser beam wavelength λ ($a >> \lambda$). In this case, the bead acts like a weak positive lens, and we can use ray optics to predict the direction of trapping forces. When the incident light passes through a high numerical aperture (NA) objective, it is concentrated into a beam with a tight waist and large gradient. There are two forces acting on the bead: a scattering force pushing the bead in the direction of incident light, and a gradient forces pulling the bead in the opposite direction.

Figure 1

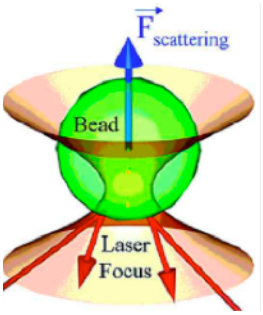

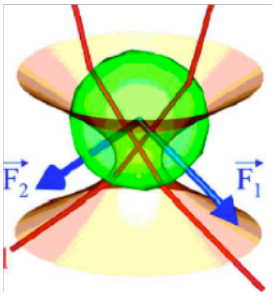

When these two forces balance each other, there is a stable trap. The gradient force is caused by the refraction of light as it passes through the bead, and the resulting

change in momentum since $F = dp/dt$. The net change in momentum must be zero, and so momentum must be transferred from the beam to the bead in the equal and opposite direction (F_1 and F_2 in Fig. 1). If the bead is off axis from the incident beam, it will refract the light such that the gradient force will move the bead back on axis (Fig. 2).

Figure 2

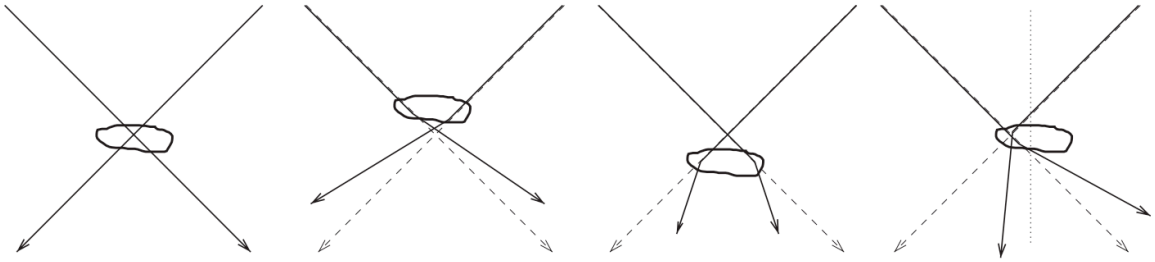

In order to get a more quantitative description of the bead behavior, we can examine the limiting case when $a << \lambda$, in the Rayleigh scattering regime. We can treat the bead as a point dipole in an inhomogeneous electric field and calculate that the scattering and gradient forces acting on the bead should be:

$$F_{\text{scatt}} = \frac{I_0 \sigma n_m}{c}, \qquad F_{\text{grad}} = \frac{2\pi\alpha}{c n_m^2} \nabla I_0,$$

$$\sigma = \frac{128\pi^5 a^6}{3\lambda^4}\left(\frac{m^2-1}{m^2+2}\right)^2 \qquad \alpha = n_m^2 a^3 \left(\frac{m^2-1}{m^2+2}\right)$$

I_0 is the incident beam intensity and m is the ratio of the refractive index of the particle to that of the medium (n_p/n_m). Plots of net axial and radial forces acting on the particle (Fig. 3) are symmetric, and show that the trap covers a finite area that is dependent on intensity and gradient of the incident beam.[2]

Figure 3

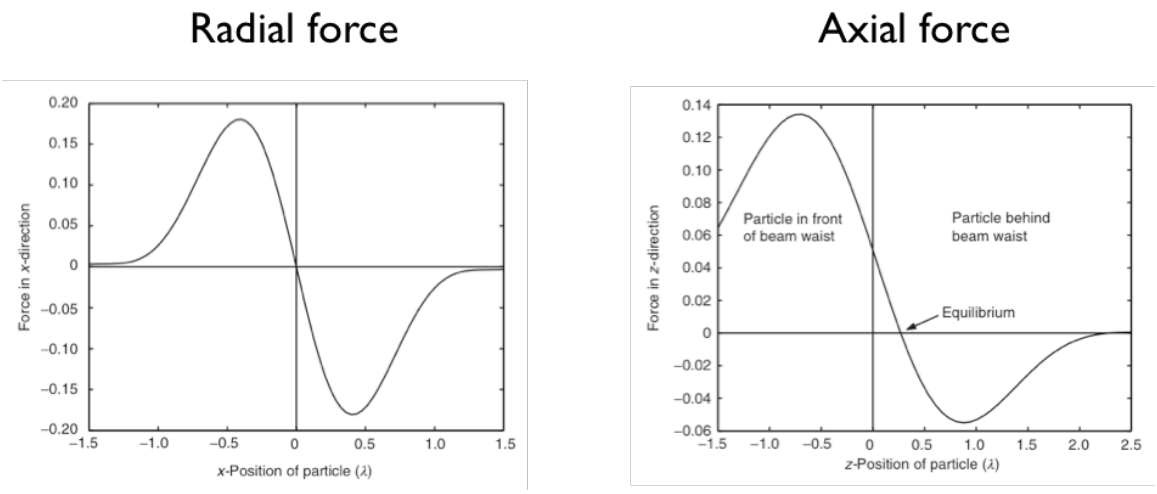

The equilibrium position along the axis parallel to the beam is distal to the narrowest part of the beam because the scattering force pushes the bead forward. Finally, the force versus distance relationship near the center of the trap is linear, which means the trap acts like a Hookean spring with F=kx, where k is the spring constant.

The Rayleigh approximation can also provide insight into the behavior of particles of different sizes (a) and refractive indices (n_p) in a fixed experimental setup (n_m = 1, λ = 1064nm, NA=1.3).

Figure 4

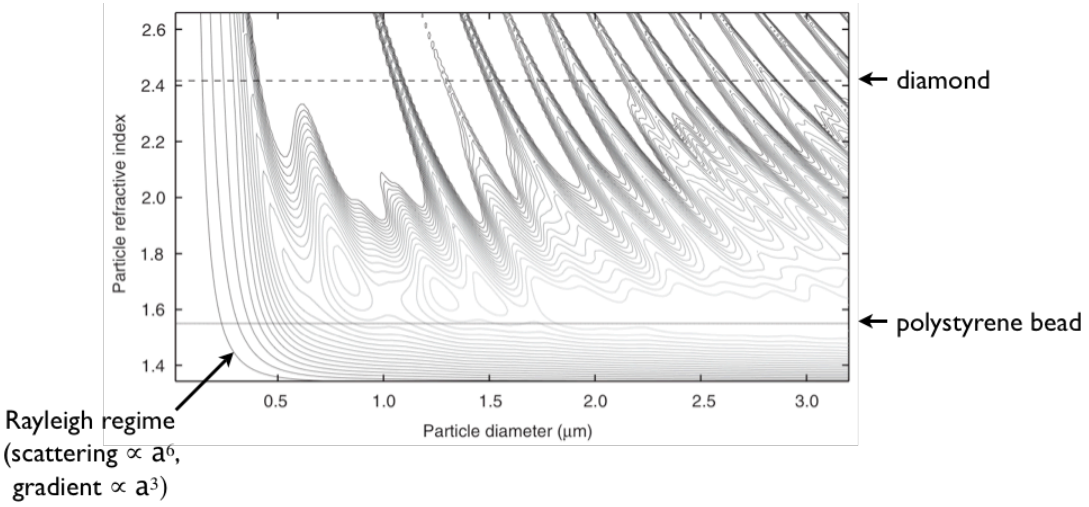

Since the scattering force is proportional to a^6 and the gradient force is proportional to a^3, small particles will be trapped regardless of their refractive index. Polystyrene beads of a wide range of sizes can be trapped, and diamond (high n_p) can in theory be trapped at sizes where the reflected beam from the front and back surfaces interferes destructively, thus reducing the scattering force.

Resolution limits

The spatio-temporal resolution of optical tweezers is limited by experimental and thermal (Brownian) noise. Experimental noise is introduced by the environment and instrument and can be minimized with careful design. We controlled thermal and vibrational noise by working in a temperature-controlled lab on an optics table floating on air hydraulics. Our sample was mounted on a stage with micromanipulators that allowed us to move it relatively smoothly in small increments. We also mounted our laser on a water-cooled platform to increase the stability of the incident beam. We could have reduced experimental noise more by

using electronic stage controls or an acousto-optic deflector (AOD) to move the trap without jarring the stage with our hands. Electronic and acoustic isolation could have been improved by moving to a more isolated lab space.

Brownian motion of the bead is unavoidable, but it is dependent on changeable parameters, and so it can be reduced through careful experimental design. The signal-to-ratio of a single trap (with no experimental noise) can be approximated as:[5]

$$SNR \leq \frac{\kappa_{tether} \Delta \ell}{\sqrt{4 k_B T B \gamma}}$$

Therefore, one can increase the SNR by decreasing T, B or γ or changing the stiffness or length of the tether (which we are not using in our setup). Decreasing the temperature T of the bath is not useful in practice because biological systems can function only in a narrow temperature range. Reducing the bandwidth B of the measurement, which demonstrates the trade-off between spatial and temporal resolution. Finally, one can reduce the drag $\gamma = 6\pi\eta a$ by decreasing the viscosity of the medium, or more feasibly, by decreasing the bead size. However, very small beads (<0.2μm) are difficult to visualize and will be trapped more weakly (optimal trapping efficiency occurs when bead diameter ~ laser wavelength)[5]. Also, it should be noted that changing the trap stiffness has no effect on the SNR because while a stiffer trap will cause a bead to thermally fluctuate less, the bead will also be less sensitive to motions of the biological system that one is attempting to measure.

Experimental setup

This project utilized an infrared (IR) laser to create an optical trap for polystyrene beads. The infrared laser path for our experiment utilized four mirrors in order to direct the beam into the back aperture of the objective. The objective is an oil-immersion objective, has a 40X magnification, with a 0.17 mm working distance and an NA of 1.30. There were, in addition, three lenses that were used to manipulate the physical beam properties. CL helped to collimate the beam to avoid power loss, while L1 and L2 provided beam expansion. In the final setup, L1 and L2 were used to expand the beam in order to fill the back aperture of the objective. L1 has a focal length of 50.8 mm and L2 has a focal length of 150 mm, resulting in a 3X beam expansion, giving the resulting beam an approximate diameter of 8 mm. The beam then passed through a dichroic mirror that is designed to pass IR light and reflect visible light, allowing for simultaneous trapping and imaging. IR filters were placed over L3 and the CCD in order to filter the IR interference from the resulting image. The imaging plane was arranged perpendicularly to the optical axis, so that the imaging plane was aligned vertically. The experimental set up can be seen in Figure 5.

Figure 5

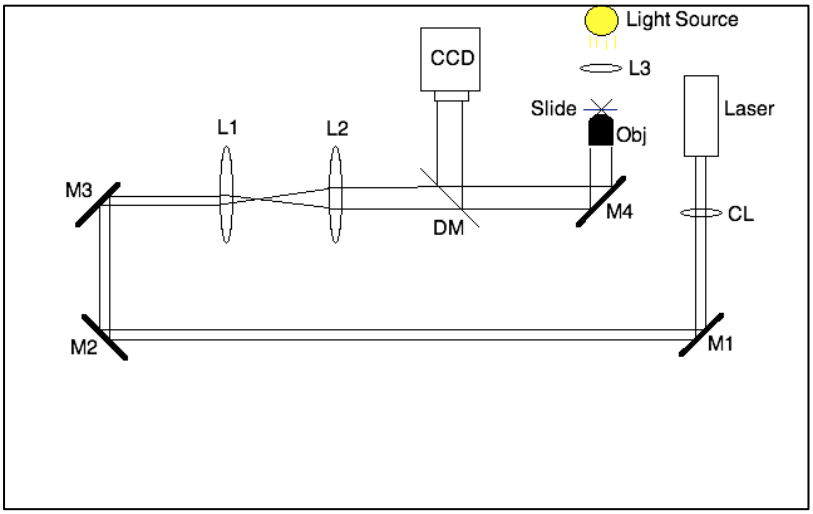

Method

The actual implementation of this setup was more difficult than expected, as many unforeseen problems arose. The primary issue with the setup shown in Figure 5 was the aligning of the optical axis: the axis for the infrared laser had to be perpendicular to that of the objective and to the table, and the dichroic mirror had to be aligned with the reflective surface facing the beam source in order to minimize interference. In addition, the IR filters used to prevent interference from the IR beam must be placed perpendicular to the imaging plane.

Although, ideally the IR laser is collimated, the reality is that the beam diverges widely throughout the optical path. For this reason, the lens CL is placed in the path in order to reduce this divergent pattern. In addition, the telescoping effect of lenses L1 and L2 help to collimate the laser and reduce divergence, which results in a sharp focus at the specimen plane. A track was used to adjust the position of L1 along the optic axis in order to minimize divergence.

The original objective we had was insufficient for trapping. As an older lens, it did not sufficiently pass light in the IR spectrum to allow for trapping. As a result, we switched it out for a newer lens that does not have the sharp decline in transmitted power that the original, 100X objective does. Although the replacement objective had a lower magnification, the resulting trap had enough power to trap 2 μm polystyrene beads.

In order to locate the proper focal plane for an optic trap, the IR filters were removed so that the IR interference patterns could be observed. An empty glass slide was then placed in the specimen plane, which was then adjusted in the z-direction until the IR focus was observed.[6] This was the location of the trap. The position was noted, and the empty slide was replaced with a specimen slide, which contained a well of polystyrene beads diluted at 1:10 or 1:100. First it was ensured that Brownian motion was observed, which indicated whether the beads were suspended in solution or stuck to the glass slide. If Brownian motion was observed, then the IR beam was turned on in order to observe trapping. Video of the trapping was captured using video capture software.

Experimental Results

Trapping was successfully achieved in both dense (Fig. 6) and sparsely populated wells of polystyrene beads. The trap location in the viewing field was manipulated both by moving the x-, y- and z-position of the stage, as well as the horizontal position of L1. Moving L1 resulted in a smoother motion of the bead since the stage was not vibrated by hand movement.

Figure 6

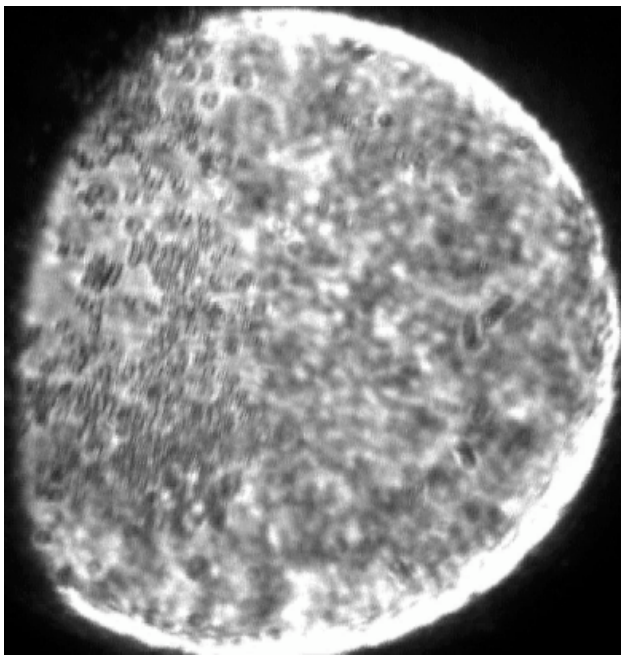

Discussion

There have been a host of advancements since Ashkin's early trapping experiments, that include exploiting asymmetries in the trapping beam to generate rotational forces and using holograms to create hundreds of traps with a single laser beam. These computer generated holograms are interference patterns placed at the entrance of the objective that change the phase of the incident beam in order to mimic multiple beams.[7]

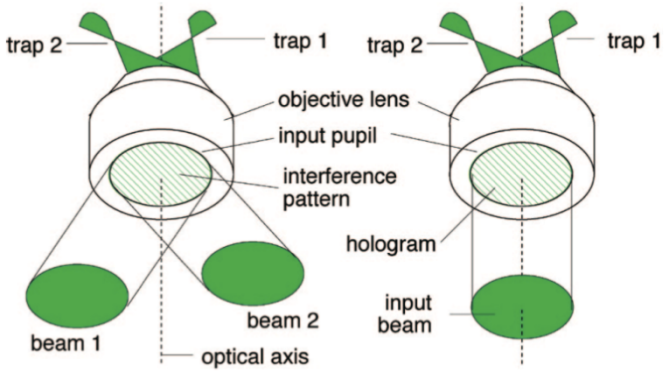

Multiple traps have been exploited to generate microfluidics devices that can be rearranged dynamically and have been used for cell sorting and biomedical diagnostics.

References

1. Neuman, K.C. and A. Nagy, *Single-molecule force spectroscopy: optical tweezers, magnetic tweezers and atomic force microscopy.* Nat Methods, 2008. **5**(6): p. 491-505.
2. Nieminen, T.A., et al., *Physics of optical tweezers.* Methods Cell Biol, 2007. **82**: p. 207-36.
3. Ashkin, A., *Acceleration and Trapping of Particles by Radiation Pressure.* Physical Review Letters, 1970. **24**(4): p. 156.
4. Ashkin, A., et al., *Observation of a single-beam gradient force optical trap for dielectric particles.* Opt. Lett., 1986. **11**(5): p. 288.
5. Moffitt, J.R., et al., *Recent advances in optical tweezers.* Annu Rev Biochem, 2008. **77**: p. 205-28.
6. Block, S.M., *Construction of Optical Tweezers*, in *Cells: A Laboratory Manual*, D.L. Spector, Editor. 1998, Cold Spring Harbor Laboratory Press: Cold Spring Harbor.
7. Grier, D.G. and Y. Roichman, *Holographic optical trapping.* Appl Opt, 2006. **45**(5): p. 880-7.